THE JOURNAL OF BIOLOGICAL CHEMISTRY Vol. 272, No. 29, Issue of July 18, pp. 17972–17980, 1997
Printed in U.S.A.

Targeted Replacement of the Mouse Apolipoprotein E Gene with the Common Human *APOE3* Allele Enhances Diet-induced Hypercholesterolemia and Atherosclerosis*

(Received for publication, December 19, 1996, and in revised form, April 24, 1997)

Patrick M. Sullivan, Hafid Mezdour‡, Yasuaki Aratani‡§, Chris Knouff, Jamila Najib¶, Robert L. Reddick‖, Steven H. Quarfordt, and Nobuyo Maeda‡‡**

*From the Department of Pathology and Laboratory of Medicine, the University of North Carolina, Chapel Hill, North Carolina 27599-7525, the ¶Institut Pasteur de Lille U-235, Lille, France, and the **Department of Medicine, Durham VA Hospital and Duke University Medical Center, Durham, North Carolina 27705*

Apolipoprotein (apo) E, a constituent of several lipoproteins, is a ligand for the low density lipoprotein receptor, and this interaction is important for maintaining cholesterol and triglyceride homeostasis. We have used a gene replacement strategy to generate mice that express the human apoE3 isoform in place of the mouse protein. The levels of apoE mRNA in various tissues are virtually the same in the human apoE3 homozygous (3/3) mice and their littermates having the wild type mouse allele (+/+). Total cholesterol and triglyceride levels in fasted plasma from the 3/3 mice were not different from those in the +/+ mice, when maintained on a normal (low fat) chow diet. We found, however, notable differences in the distribution of plasma lipoproteins and apolipoprotein E between the two groups: β-migrating lipoproteins and plasma apoB100 levels are decreased in the 3/3 mice, and the apoE distribution is shifted from high density lipoproteins to larger lipoprotein particles. In addition, the fractional catabolic rate of exogenously administered remnant particles without apoE was 6-fold slower in the 3/3 mice compared with the +/+ mice. When the 3/3 and +/+ animals were fed a high fat/high cholesterol diet, the 3/3 animals responded with a dramatic increase (5-fold) in total cholesterol compared with the +/+ mice (1.5-fold), and after 12 weeks on this same diet the 3/3 animals developed significantly (at least 13-fold) larger atherosclerotic plaques in the aortic sinus area than the +/+ animals. Thus the structural differences between human APOE3 and mouse ApoE proteins are sufficient to cause an increased susceptibility to dietary-induced hypercholesterolemia and atherosclerosis in the 3/3 mice.

Apolipoprotein (apo)[1] E is important for the transport of cholesterol and triglyceride throughout the body. It is an amphipathic protein that stabilizes the structure of lipoprotein particles via its ability to bind lipid, and it functions as a ligand for lipoprotein receptors, such as the low density lipoprotein receptor (LDLR) and the low density lipoprotein receptor-related protein (1–3). ApoE is a major protein component of chylomicron remnants, very low density lipoproteins (VLDL), and intermediate density lipoproteins (IDL), but it is not present on low density lipoproteins (LDL). ApoE is also enriched in a subclass of high density lipoproteins (HDL) and functions as an effective ligand for their binding to the LDLR (4).

The human *APOE* gene is located on chromosome 19 (5) as part of an apolipoprotein cluster that also includes the genes encoding *APOCI*, *APOCII*, and *APOCIV* (6). Multiple tissue-specific enhancers and negative elements have been identified in the region proximal to the gene (7). A distal enhancer, the hepatic control region, that is required for liver expression is located 15 kb downstream of the gene (8, 9). The liver synthesizes approximately 70% apoE found in the body and 20% is found in the brain, and the remainder is synthesized in several tissues including the spleen, lung, heart, ovary, testis, kidney, and skin (10, 11).

Three major *APOE* alleles, ε2, ε3, and ε4, occur in humans at frequencies of 7.3, 78.3, and 14.3%, respectively (12). These three alleles are distinguished by coding differences at positions 112 and 158 (13). The most common isoform, apoE3, has a cysteine at position 112 and an arginine at position 158; the apoE2 isoform has a cysteine at both positions, whereas the apoE4 isoform has an arginine at both positions. Functionally, the three isoforms differ in their affinity for the LDLR, with apoE3 and E4 exhibiting 100% binding and apoE2 displaying only 1% normal binding affinity (14). Despite the lower affinity of apoE2 for the LDLR, individuals homozygous for ε2 typically have lower than normal plasma cholesterol levels, except for the fraction of homozygotes (5–10%) who develop type III hyperlipoproteinemia (15). Individuals homozygous for ε4 have higher total plasma cholesterol and LDL cholesterol compared with ε3 homozygotes and are at increased risk for developing coronary artery disease (16). The ε4 allele is also associated with the development of Alzheimer's disease (17, 18).

ApoE isoform-specific effects are important in the etiology of atherosclerosis and other diseases, but appropriate animal models to rigorously investigate these effects are currently

* This work was supported by a National Institute of Health Grant HL42630. The costs of publication of this article were defrayed in part by the payment of page charges. This article must therefore be hereby marked "*advertisement*" in accordance with 18 U.S.C. Section 1734 solely to indicate this fact.

‡ Supported in part by fellowships from ARCOL, France, and the Uehara Memorial Foundation, Japan, respectively.

§ Current address: Yokohama City University, Kihara Institute for Biological Research, Yokohama 244, Japan.

‖ Current address: Dept. of Pathology, University of Texas, San Antonio, TX 78284-7750.

‡‡ To whom correspondence should be addressed. Tel.: 919-966-6916; Fax: 919-966-8800.

[1] The abbreviations used are: apo, apolipoprotein; LDLR, low density lipoprotein receptor; VLDL, very low density lipoprotein; IDL, intermediate density lipoprotein; LDL, low density lipoprotein; R, receptor; HDL, high density lipoprotein; HSPG, heparan sulfate proteoglycans; 3/3, mice homozygous for human apoE3 allele; 3/+, mice heterozygous for human apoE3; +/+, mice homozygous for wild type mouse apoE allele; kb, kilobase; ES cell, embryonic stem cell; TC, total cholesterol; ELISA, enzyme-linked immunosorbent assay; hu, human; FPLC, fast protein liquid chromatography; PAGE, polyacrylamide gel electrophoresis.

lacking. To date, transgenic animals made by pronuclear injection of human DNA have been used to study these effects, but this method produces mice with varying levels of transgene expression due to differences in chromosomal location and copy number, and expression of the endogenous mouse apoE complicates the interpretation of the data (19–24, 47). To overcome these difficulties we have used targeted gene replacement to generate mice that express only the human apoE3 isoform at levels that are in the physiological range. In these mice the coding sequences for mouse *apoE* were replaced with sequences coding for human *APOE3* without disturbing any of the known regulatory sequences. This replacement results in animals with expression of human apoE mRNA, identical in tissue distribution and levels, to that of mouse apoE mRNA in wild type animals.

We here describe the essentially normal cholesterol and triglyceride levels of mice homozygous for human apoE3 (3/3) when maintained on a normal (low fat) mouse chow diet but show that they are markedly more susceptible to diet-induced atherosclerosis than their wild type littermates (+/+).

EXPERIMENTAL PROCEDURES

Targeting Construct—The targeting construct was made by inserting into a pPNT vector (25), a 4.1-kb *Sac*I human genomic fragment isolated from a plasmid, pHEG-1 (20), kindly provided by Dr. John Taylor at the University of California, San Francisco. This fragment contains the 3′ part of intron 1 (723 base pairs), exons 2–4 of the human *APOE3* gene, and 1.5 kb of 3′-flanking DNA. A 5.3-kb *Eco*RI-*Sac*I strain 129 mouse genomic fragment containing sequences upstream of the mouse *apoE* gene including exon 1 and the 5′ part of intron 1 (376 base pairs) was inserted 5′ to the human *APOE3* fragment. A 1.4-kb *Pvu*I-*Kpn*I strain 129 mouse genomic fragment containing the 3′-half of exon 4 and 3′-flanking sequence was inserted downstream of the neomycin-resistant gene in pPNT (see Fig. 1, *below*).

Generation of Homozygous Human apoE3 Mice—A subclone (BK4) of mouse strain 129 embryonic stem (ES) cell line, E14TG2a, was cultured and electroporated with the human apoE3 targeting construct as described previously (26). Targeted ES cell clones were identified by Southern blot analysis. Chimeras were generated and mated with C57BL/6J (B6) mice. F2 generation mice were used for all of the experiments described. Mice were kept on a normal (low fat) chow diet consisting of 5% (w/w) fat and 0.022% (w/w) cholesterol (Prolab RMH 3000, number 5P76, St. Louis, MO) or on an atherogenic diet that contains 15.8% (w/w) fat, 1.25% (w/w) cholesterol, and 0.5% (w/w) sodium cholate (TK 88051, Teklad Premier, Madison, WI).

Plasma Lipid Measurements—All lipid measurements were performed on mice between the age of 8 and 20 weeks. Animals were fasted overnight (approximately 16 h), anesthetized with Avertin, and 150 μl of blood was collected from the retro-orbital sinus into tubes containing 8 mM EDTA, 1 μg/ml aprotinin (Boehringer Mannheim), and 1 μg/ml gentamycin, and stored on ice. Plasma was removed after centrifugation at 8,000 $\times$ *g* for 10 min at 4 °C, and total cholesterol and HDL cholesterol were measured using diagnostic CII kits (Wako, Richmond, VA) according to the manufacturer's instructions. Triglyceride levels were measured using an enzymatic kit (Sigma).

Plasma Lipoprotein Analysis—Within 1 h of blood collection, 1 μl of plasma was electrophoresed in precast 1% agarose gels (Ciba Corning Diagnostics Corp., Palo Alto, CA), and neutral lipids were visualized by Fat Red 7B staining (Sigma). One ml of pooled plasma from 10 mice (100 μl each) was separated by sequential density ultracentrifugation into seven fractions ranging in densities from <1.006 g/ml to >1.21 g/ml, using the procedure described by de Silva *et al.* (27). Total lipoproteins were isolated from plasma at a density <1.21 g/ml. Lipoprotein fractions were dialyzed against 10 mM Tris, pH 7.4, 1 mM EDTA, 150 mM NaCl before electrophoresis in a 3–20% denaturing SDS-PAGE gel (27). Plasma (100 μl) from either individual or pooled samples were separated by gel filtration chromatography using a Superose 6 HR10/30 column (Pharmacia Biotech Inc.). Immunoblot analysis of FPLC fractions (2 μl) electrophoresed in precast 1% agarose gels was performed with antibodies described below.

Northern Blot Analysis—Total RNA was extracted from several tissues according to the method of Chomczynski and Sacchi (28) using RNAzol™ B (Tel-test, Friendswood, TX). Total RNA (20 μg) was electrophoresed in a 1% agarose gel after denaturation with a glyoxal/Me_2SO mixture (29). RNA was transferred to a Hybond membrane (Amersham Corp.) and hybridized overnight at 42 °C in 50% formamide, 5 $\times$ SSC, 1 $\times$ Denhardt's solution, 100 μg of salmon sperm DNA, 30 mM sodium phosphate, pH 6.5, and 10% dextran sulfate; the probe was a mouse exon 4 DNA fragment labeled with [^{32}P]dCTP. The blot was washed in 3 $\times$ SSC, 0.1% SDS for 10 min at 37 °C and then 0.1 $\times$ SSC, 0.1% SDS for 10 min at 65 °C. The blot was exposed to preflashed Kodak XAR film for 20 h.

ApoE Enzyme-linked Immunosorbent Assay—Human APOE in mouse plasma was measured with a sandwich-type enzyme-linked immunosorbent assay (ELISA) essentially as described (30). A mouse anti-human apoE monoclonal antibody, E01 (α huE (m)) (30), was used as the capture antibody and a goat anti-human apoE antibody (α huE (p)) (Calbiochem) as the detecting antibody. The α huE (p) antibody cross-reacts with mouse apoE at a low level. The α huE (m) antibody has been shown to react with human APOE in all classes of lipoprotein particles (30) and does not cross-react with mouse ApoE. Values were determined with a standard curve made with pooled human plasma whose apoE levels were determined against purified recombinant human apoE3 (number 178475, Calbiochem) and validated against an international calibrator (Dr. N. Rifai, Childrens Hospital, Boston, MA).

Mouse ApoE was measured in a similar manner using a purified rabbit anti-mouse apoE antibody (α muE (m)) (10 μg/ml) raised against a mouse apoE peptide (residues 179–241) for the capture antibody. The same antibody conjugated to horseradish peroxidase was used for detection with chromagen. The mouse peptide (residues 179–241) was used as a standard for determining the concentration of mouse ApoE.

Western Blot Analysis—Fasted whole plasma (1 μl) was electrophoresed in a 4–20% denaturing SDS-PAGE gel or in a 1% agarose gel, transferred to an Immobilon P membrane (Millipore Corp., Bedford, MA), and reacted with all three anti-apoE antibodies described above. Immunoreactive proteins were visualized with a horseradish peroxidase conjugate using an enhanced chemiluminescence kit (Amersham Corp.). Western blots for the analysis of apoB were made similarly using 4% SDS-PAGE and rabbit anti-mouse apoB sera (gift from Dr. Steven Young, University of California, San Francisco).

Clearance Assay—Four apoE (−/−) mice were injected with 20 μg of free cholesterol containing 2.5 μCi of 4-^{14}C-labeled cholesterol dispersed in an egg lecithin/free cholesterol (1:1 molar ratio) mesophase. The apoE (−/−) β-VLDL fraction was isolated 36 h later by centrifugation at 1.010 g/ml. More than 72% of the tracer was in the cholesterol ester fraction (31). Three mice in each group (apoE−/−, 3/3, and +/+) were injected with the labeled apoE (−/−) β-VLDL. The fractional catabolic rates and their variances were determined up to 4 h as described previously (31).

Evaluation of Atherosclerotic Lesions—Female mice that had been fed a high fat diet for 3 months were sacrificed by Avertin overdose after a 16-h fast. The thoracic cavity was opened, and the heart and vascular system were perfused with 4% paraformaldehyde in phosphate-buffered saline, pH 7.4, under physiological pressure. Segments of the proximal aorta and aortic sinus were embedded, sectioned, and stained as described previously (32). Morphometric evaluations of lesion size were made using the NIH image (version 1.41) software.

Statistical Analysis—The significance of differences between means was tested by using a two-tailed unpaired Student *t* test or a nonparametric Mann-Whitney *U* test.

RESULTS

Replacement of the Mouse apoE Gene with the Human APOE3 Allele—The targeting strategy used to replace the mouse apoE coding exons 2–4 with the human counterpart is illustrated in Fig. 1. Homologous recombination between the targeting construct (Fig. 1*B*) and the endogenous mouse *apoE* locus (Fig. 1*A*) results in a chimeric gene (Fig. 1*C*) where all the mouse coding sequences have been replaced with sequences coding for human *APOE3*. This chimeric locus retains all normal mouse regulatory sequences in addition to the non-coding mouse exon one. Identification of correctly modified embryonic stem (ES) cells was by Southern blot analysis with a mouse exon 1 or exon 4 probe (data not shown); ES cell DNA digested with *Eco*RI and hybridized with the mouse exon 1 probe revealed an 8.3-kb endogenous band and a 7.8-kb targeted band confirming the correct modification of the 5′ region; ES cell DNA digested with *Hin*dIII and hybridized with mouse exon 4 probe revealed a 7.5-kb endogenous band and a 15-kb targeted

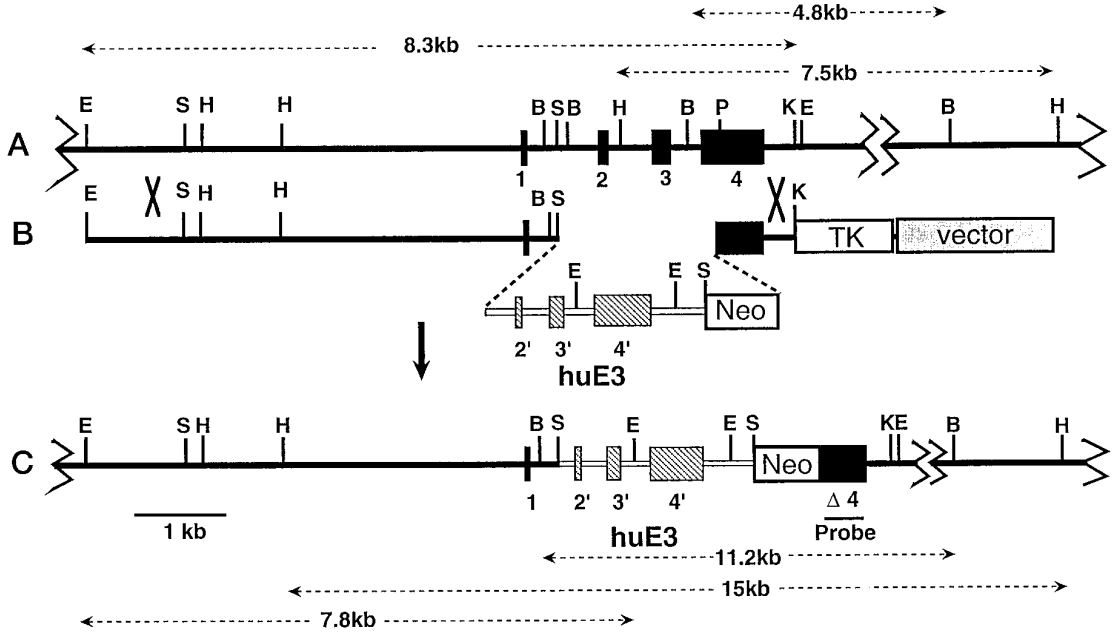

FIG. 1. **Replacement of the mouse *apoE* gene with the human *APOE3* gene.** *A*, genomic organization of the mouse *apoE* gene containing exons 1–4 (*black boxes*). *B*, the apoE3 targeting construct containing the 5′ and 3′ arms of mouse homology (*black line* and *boxes*) interrupted by the human apoE3 gene (*hatched boxes* 2′, 3′, and 4′, labeled *huE3*). The neomycin-resistant (*Neo*) and thymidine kinase (*TK*) genes are for selection of the targeted ES cells, and pPNT is the plasmid vector. *C*, the resulting chimeric gene now encoding human apoE3. The mouse exon 4 probe (*Probe*) was used to detect the targeted allele. Sizes of diagnostic fragments are shown (*dashed lines*). Sites are as follows: *E*, *Eco*RI; *S*, *Sac*I; *H*, *Hin*dIII; *P*, *Pvu*I; *K*, *Kpn*I; *X*, *Xba*I; *B*, *Bam*HI.

band confirming correct modification of the 3′ region. The modified locus was transmitted to the F1 generation from chimeras that were made from one of the targeted cell lines. All F1 matings produced normal litter sizes with a normal Mendelian segregation pattern of the modified locus. Genotypes of F2 animals were determined using Southern blot analysis of tail DNA digested with *Bam*HI (Fig. 2*A*). The nucleotide sequence for codon 112 (TGC) and codon 158 (CGC) in a 3/3 mouse was confirmed using allele-specific PCR (33) on tail DNA.

Human apoE3 Levels in Whole Plasma—To confirm the presence of human APOE protein in the mice, plasma (1 μl) from 3/3, 3/+, +/+ mice, and a human (hu) were electrophoresed in a 4–20% gradient denaturing SDS-PAGE gel. Western blot analysis with anti-human apoE antisera (α huE (p)), which slightly cross-reacts with mouse ApoE, showed that human APOE (34, 200 Da) in 3/3 plasma migrates at the same rate as apoE in human plasma and slightly slower than the mouse apoE (32, 600 Da) in +/+ plasma (Fig. 2*B*). The absence of mouse ApoE in the 3/3 plasma was confirmed by Western blot analysis with an anti-mouse apoE antibody (α mu (m)), which shows that mouse ApoE is present only in the +/+ and 3/+ samples and not in the 3/3 plasma. In contrast, the anti-human apoE monoclonal antibody (α huE (m)), which does not cross-react with mouse ApoE, shows that human APOE was present only in 3/3, 3/+, and human plasma and not in the +/+ plasma (Fig. 2*B*). Western blotting of plasma from two 3/3 mice in a 4–20% nonreducing SDS-PAGE gel showed that human APOE3 homodimer was present at less than 5% monomeric E3 (Fig. 2*C*).

The concentration of apoE in 3/3 plasma (1.30 ± 0.47 mg/dl) as determined by ELISA was very similar to the levels (1.13 ± 0.23 mg/dl) found in +/+ plasma (see Table I below).

Tissue Distribution of apoE mRNA—Total RNA was extracted from several tissues including skin (*Sk*), spleen (*Sp*), kidney (*Ki*), small intestine (*Si*), stomach (*St*), heart (*He*), testis (*Te*), muscle (*Mu*), lung (*Lu*), liver (*Li*), submandibular gland (*Su*), and brain (*Br*) from a 3/3 male mouse and a wild type +/+ male mouse. Northern blot analysis with a mouse exon 4 probe

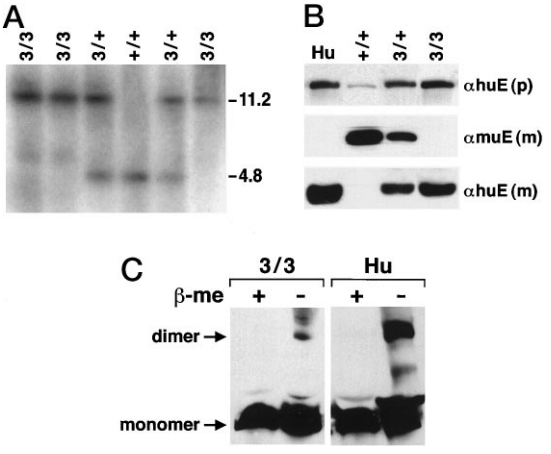

FIG. 2. **Southern and Western blot analysis.** *A*, Southern analysis with a mouse exon 4 probe to identify F2 mice carrying the targeted allele. An 11.2-kb hybridizing *Bam*HI fragment indicates the presence of the human *APOE3* allele. A 4.8-kb hybridizing *Bam*HI fragment indicates the presence of the mouse *apoE* allele. *B*, fasted whole plasma (1 μl) was electrophoresed in a 4–20% denaturing SDS-PAGE gel, and the proteins were transferred to an Immobilon P membrane and incubated with either an anti-human apoE antisera (α huE (p)) that weakly cross-reacts with mouse apoE (*top panel*) or with an anti-mouse apoE antibody (α muE (m)) (*middle panel*) or with an anti-human apoE monoclonal antibody (α huE (m)) (*bottom panel*) that does not cross-react with mouse apoE. *C*, fasted whole plasma (1 μl) was electrophoresed in a 4–20% SDS-PAGE gel, and the proteins were transferred to an Immobilon P membrane and incubated with α huE (p) antiserum in the presence (+) or absence (−) of β-mercaptoethanol (β-*me*). The abbreviations used are: *Hu*, human sample; *3/3*, sample from homozygous human apoE3 mouse; *3/+*, heterozygous sample; +/+, wild type sample.

was used to compare the levels of apoE mRNA in the two types of animal (Fig. 3). This probe hybridizes equally well to the human gene and the mouse gene under the conditions used. A β-actin probe was hybridized to the same blot after removal of the apoE probe (*lower panels* in Fig. 3) to assess the amount of mRNA loaded in each group. In agreement with previous reports (10, 11) apoE mRNA expression was highest in the liver

TABLE I

Plasma lipid profiles and apoE concentration in mice fed a normal and a high fat diet

Data are means ± S.D. of fasted mice receiving chow (C) or high fat (HF) diet. Parentheses show the number of mice. TG, triglyceride.

	Genotype	Diet	TC	TG	HDL-cholesterol	Human apoE3	Mouse apoE
			mg/dl	*mg/dl*	*mg/dl*	*mg/dl*	*mg/dl*
Females	3/3	C	67 ± 18 (30)	35 ± 12 (26)	46 ± 11 (26)	1.30 ± 0.47 (10)	
		HF	350 ± 207 (17)[a]	29 ± 22 (15)	22 ± 11 (14)	10.80 ± 5.60 (8)[a]	
	+/+	C	73 ± 20 (30)	43 ± 15 (26)	53 ± 15 (23)		1.13 ± 0.23 (6)
		HF	111 ± 44 (17)[b]	21 ± 7 (14)	23 ± 15 (13)		1.11 ± 0.34 (5)
Males	3/3	C	104 ± 22 (15)[c]	39 ± 16 (13)	54 ± 19 (7)		
	+/+	C	95 ± 16 (15)	41 ± 17 (14)	52 ± 15 (7)		

[a] $p < 0.01$ *versus* 3/3 females on chow.
[b] $p < 0.001$ *versus* 3/3 females on high fat.
[c] $p < 0.001$ *versus* female 3/3.

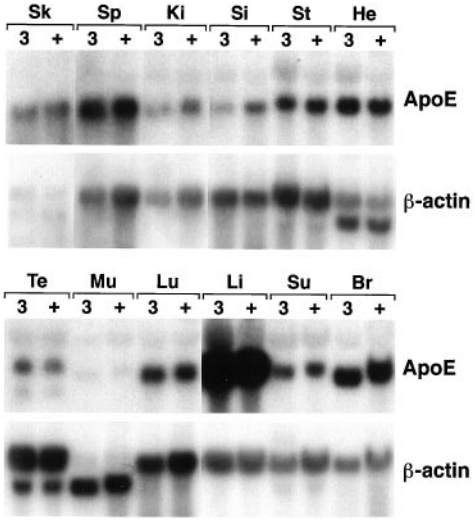

FIG. 3. **Northern blot analysis of total RNA from various tissues.** Total RNA (20 μg) was electrophoresed in a 1% gel, blotted, and then hybridized to a mouse apoE exon 4 probe, as indicated. The same filter was rehybridized with a β-actin probe. *3* identifies lanes containing RNA from human apoE3 mice; + identifies lanes containing RNA from wild type mice; *Sk*, skin; *Sp*, spleen; *Ki*, Kidney; *Si*, small intestine; *St*, stomach; *He*, heart; *Te*, testis; *Mu*, muscle; *Lu*, lung; *Li*, liver; *Su*, submandibular gland; *Br*, brain.

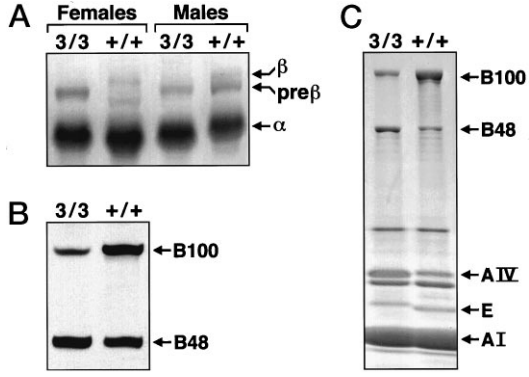

FIG. 4. **Analysis of plasma lipoproteins.** *A*, fasted plasma (1 μl) from males and females maintained on a normal (low fat) chow diet was electrophoresed in a 1% agarose gel and stained with Fat Red 7B. The positions of the α-, β-, and pre-β-lipoproteins are indicated. *B*, Western analysis of fasted plasma (1 μl) from female mice using a denaturing 4% SDS-PAGE gel with an anti-apoB antisera. The positions of the apoB100 and 48 proteins are indicated. Samples are from 3/3, homozygous human apoE3 mice, and from +/+, wild type mice. *C*, total lipoproteins (density <1.21 g/ml) pooled from five female 3/3 and four +/+ mice were electrophoresed in a 3–20% SDS-PAGE gel and stained with Coomassie Brilliant Blue. The positions of the apolipoproteins are as indicated.

and second in the brain, with lesser amounts in other tissues. No apoE mRNA was detected in muscle. The expression of apoE mRNA in the 3/3 and +/+ animals was essentially indistinguishable in all tissues analyzed, with the exception of small intestine which had reduced levels of apoE mRNA in the 3/3 animals compared with +/+ mice. This Northern blot analysis clearly demonstrates that the modified locus containing human apoE3 coding sequences and the wild type mouse gene are expressed at virtually identical levels in all tissues.

Plasma Lipids and Lipoproteins in Mice Fed Normal Chow—The levels of total cholesterol (TC), triglycerides, and HDL cholesterol in female mice fed a normal (low fat) chow diet were determined in plasma obtained after a 16-h fast (Table I). There was no difference in TC levels between the 3/3 mice (67 ± 18 mg/dl, $n = 30$) and the +/+ controls (73 ± 20 mg/dl, $n = 30$), in striking contrast to the total cholesterol levels previously found in apoE-deficient mice on the same diet (541 ± 220 mg/dl, 32). The TC levels in males were higher than females ($p = 0.0001$), but again there were no differences between the 3/3 and the +/+ group. Triglyceride and HDL cholesterol levels in the 3/3 mice and the +/+ mice were also very similar (Table I).

Fasted wild type (+/+) plasma lipoproteins migrate as three distinct bands designated α (HDL), β (LDL), and pre-β (VLDL) using agarose gel electrophoresis (Fig. 4*A*). Plasma from fasted 3/3 mice, on the other hand, showed an increase in the pre-β band and the absence of β-migrating lipoproteins relative to the +/+ samples. These differences were observed in the plasma of both male and female 3/3 mice. The amount of α-migrating particles in the 3/3 and +/+ mice were the same. These results suggest that the 3/3 mice have slightly increased amounts of VLDL/IDL remnants and a reduction of LDL particles.

To determine the amount of apoB100 relative to apoB48, equal amounts of whole plasma from a 3/3 and a +/+ female mouse were separated in a 4% SDS-PAGE gel, blotted, and reacted with anti-mouse apoB sera (Fig. 4*B*). A densitometric scan of the autoradiograph showed that the 3/3 sample had a B100:B48 ratio of 1:3 compared with a B100:B48 ratio of 1:0.8 in the +/+ sample. In a separate experiment total lipoproteins (density <1.21 g/ml) were isolated from pooled plasma from five female 3/3 mice and four +/+ mice and electrophoresed in a 3–20% SDS-PAGE gel. Coomassie Brilliant Blue staining of the gel (Fig. 4*C*) showed that plasma apoB100 levels in the 3/3 mice were greatly reduced compared with the +/+ mice and that apoB48 levels were higher in the 3/3 mice compared with the +/+ mice.

Different Distribution of Human and Mouse Apolipoprotein E—Individual plasma samples and pooled ($n = 10$) plasma samples were separated by gel filtration chromatography on a Superose 6B column for the determination of cholesterol, triglyceride, and apoE distribution. The distribution of cholesterol

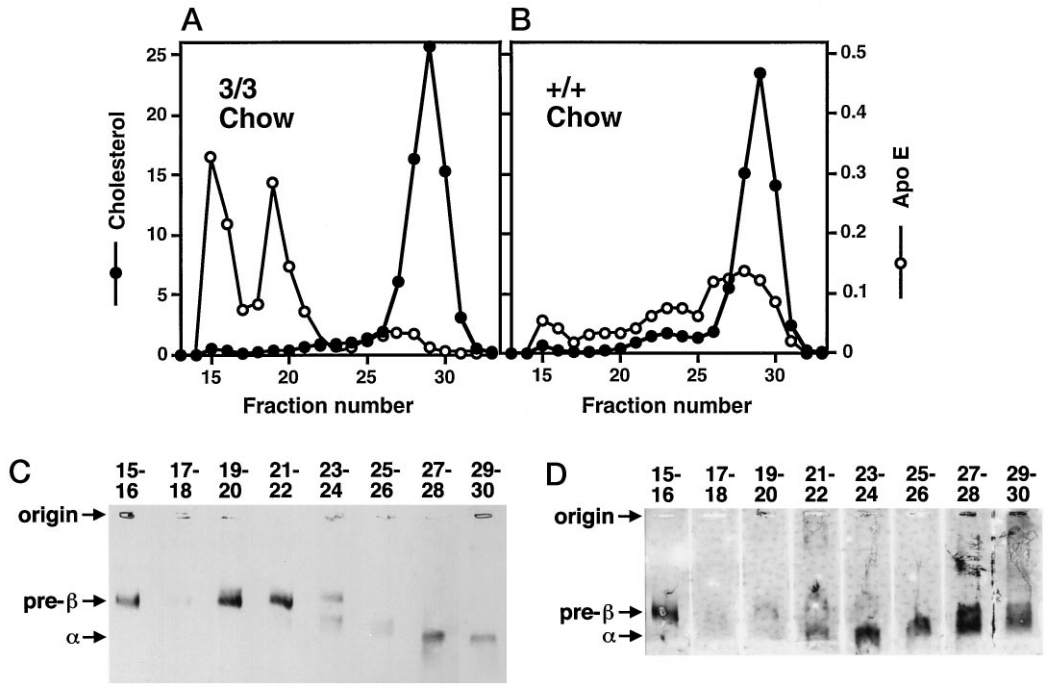

FIG. 5. **Distribution of cholesterol and apoE in mice fed normal chow.** *A* and *B*, pooled plasma from 10 mice were fractionated by gel filtration chromatography on a Superose 6B column. 0.5-ml fractions were collected, and cholesterol was measured in μg/fraction. ApoE (μg/fraction) was measured using an ELISA with antibodies specific for human (α huE (m)) (*A*) or mouse apoE (α muE (m)) (*B*). *C* and *D*, Western blot analysis of FPLC fractions (*C*, 3/3 and *D*, +/+) electrophoresed in 1% agarose gels and incubated with (α huE (p)) antiserum that cross-reacts with mouse apoE.

(*solid circles* in Fig. 5, *A* and *B*) was nearly identical for the 3/3 and +/+ mice except for a small decrease in fractions 21–24 in the 3/3 group. This decrease in LDL cholesterol agrees with the agarose gel electrophoresis results described above. Triglyceride distribution was essentially the same for both groups (data not shown) with the largest percentage of triglyceride present in fractions 14–16.

Contrary to the identical distribution of lipids, the distribution of apoE (*open circles* in Fig. 5, *A* and *B*) in the 3/3 and +/+ mice was markedly different as determined by ELISA with mouse- and human-specific antibodies. The majority of apoE in +/+ mice is present in the HDL region (fractions 26–31) with only a minor amount present in the VLDL (fractions 14–17) and IDL-LDL regions (fractions 18–25) (Fig. 5*B*). Western blot analysis of +/+ FPLC fractions electrophoresed in an agarose gel using the α-huE (p) antisera support the results obtained by ELISA (Fig. 5*D*). However in the 3/3 mice the majority of apoE is present in two very distinct peaks where VLDL (fractions 14–17) and IDL species (fractions 18–21) typically elute (Fig. 5*A*). Western blots of an agarose gel with each FPLC fraction are in agreement with the apoE3 distribution as determined by ELISA (Fig. 5*C*). SDS-PAGE gel electrophoresis of lipoproteins fractionated by sequential density ultracentrifugation (Fig. 6*A*) showed that apoE3 in the 3/3 mice was found predominantly in the lower density fractions, $d < 1.04$ g/ml. No major differences were detectable in the distributions of apolipoproteins AI in the 3/3 and +/+ samples and the apoC's after SDS-PAGE of fractions separated by sequential density ultracentrifugation (Fig. 6*A*).

The IDL-like peak in 3/3 plasma is particularly noteworthy since cholesterol and triglyceride in these fractions are very low. These IDL-like particles, enriched in apoE3, most likely represent VLDL/chylomicron remnants since agarose gel electrophoresis of FPLC fractions followed by Western blotting with α huE (p) antisera demonstrated that the majority of apoE3 was associated with particles migrating at the pre-β-position, and association of apoE3 with large HDL particles at the α-position was minimal (Fig. 5*C*). FPLC analysis of plasma after immunoprecipitation with an anti-mouse apoB antibody

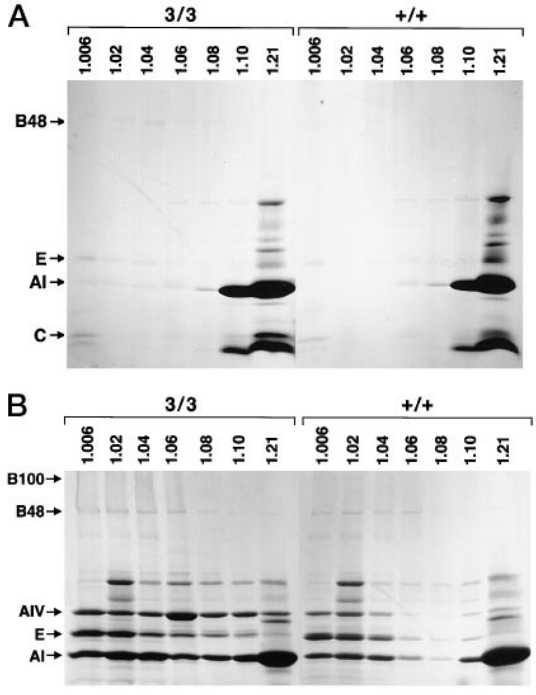

FIG. 6. **Distribution of apolipoproteins in mice fed either a normal or high fat diet.** *A*, pooled plasma from 10 mice fed normal chow were fractionated by sequential density ultracentrifugation, and each fraction was electrophoresed in a denaturing SDS-PAGE 3–20% gradient gel and stained with Coomassie Brilliant Blue. Density fractions are: *1.006*, <1.006 g/ml; *1.02*, 1.006–1.02 g/ml; *1.04*, 1.02–1.04 g/ml; *1.06*, 1.04–1.06 g/ml; *1.08*, 1.06–1.08 g/ml; *1.10*, 1.08–1.10 g/ml; *1.21*, 1.10–1.21 g/ml. *B*, the same as above except mice were fed a high fat diet for 3 months.

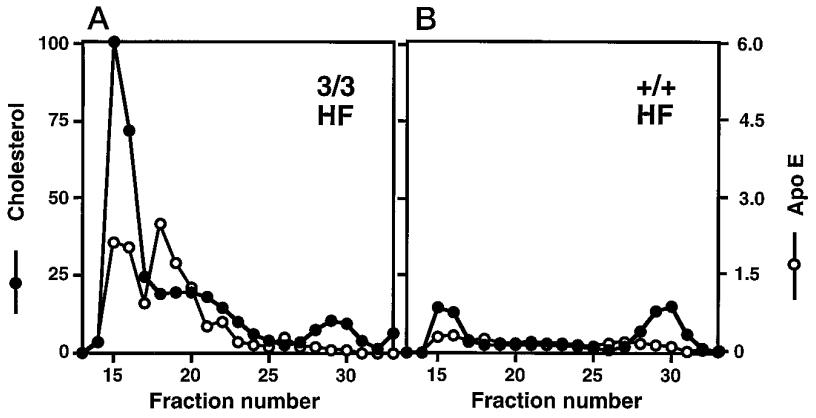

FIG. 7. **Distribution of cholesterol and apoE in mice on a high fat (*HF*) diet.** *A* and *B*, plasma from 10 mice were pooled from each group, and their lipoproteins were fractionated by gel filtration chromatography on a Superose 6B column. 0.5-ml fractions were collected, and cholesterol was measured in μg/fraction. ApoE (μg/fraction) was measured using an ELISA with antibodies specific for human (α huE (m)) (*A*) or mouse apoE (α muE (m)) (*B*).

confirms that the IDL-like particles contain apoB (data not shown). Interestingly, FPLC analysis of plasma from mice heterozygous for human apoE3 (3/+) showed a shift of the second apoE3 peak to fractions 21–25, suggesting that the co-presence of mouse ApoE reduces the size of remnant particles where apoE3 accumulates (data not shown). An increase in mouse ApoE, associated with larger particles, is also evident in the heterozygote although approximately half of mouse ApoE was still found associated with HDL.

Response to an Atherogenic Diet—The same 3/3 (n = 12) and +/+ (n = 12) female mice used to measure lipid profiles on normal chow were fed an atherogenic diet for 8 weeks to assess any change in response to diet between the two groups. One +/+ animal showed significant weight loss with a yellow colored plasma during the diet study and was excluded. The 3/3 mice responded with a 5-fold increase in cholesterol (350 ± 207 *versus* 67 ± 18 mg/dl), whereas the cholesterol in control mice increased about 1.5-fold (111 ± 44 *versus* 73 ± 20 mg/dl) (Table I). Triglyceride levels in the 3/3 and +/+ mice were reduced by 18 and 50%, respectively. HDL cholesterol levels were reduced in both groups of mice to about the same extent (approximately 50%). Agarose gel electrophoresis of plasma from both types of animals showed a decrease in α-migrating particles and an increase in pre-β-migrating particles consistent with total lipid measurements (data not shown). These results suggest that there is a marked increase in remnant particles with concurrent reduction in HDL in response to the atherogenic diet in both types of mice, but the extent of increase in the 3/3 mice is much larger.

The elution profile in a Superose 6 gel filtration column of 3/3 plasma (Fig. 7*A*) showed that the majority of the (highly elevated) cholesterol was in the VLDL-IDL fractions, whereas in the +/+ group (modestly increased) cholesterol was distributed equally between the VLDL and HDL fractions (Fig. 7*B*). As expected in the +/+ mice, the distribution of apoE followed that of cholesterol (Fig. 7*B*). The apoE distribution pattern in the 3/3 animals was highly unusual and was similar to that seen when the same animals were fed a normal chow diet; again two distinct classes of lipoproteins in the VLDL and IDL range were associated with human APOE (Fig. 7*A*). There was a large increase in plasma apoE in the 3/3 animals (10.80 ± 5.60 *versus* 1.30 ± 0.47 mg/dl) compared with no increase in the +/+ animals (1.11 ± 0.34 *versus* 1.13 ± 0.23 mg/dl) between the two diets (Table I).

The distributions of several other plasma apolipoproteins were also different between the 3/3 and +/+ mice fed the high fat diet (Fig. 6*B*). A comparison of the apolipoprotein distribution among density fractions by SDS-PAGE in Fig. 6, *A* (normal chow) and *B* (high fat), revealed a marked increase on the high fat diet of apoE, AI, and AIV mainly in the 1.006–1.04 g/ml fractions in the +/+ mice. In contrast the 3/3 mice showed increases in these proteins over the whole density range. Of particular interest is the increase of apoAI in the $1.006 < d < 1.04$ fraction, and apoAIV in the $1.04 < d < 1.06$ fraction in the 3/3 mice. The amount of apoB48 was increased in the 3/3 mice compared with +/+ mice, but their distribution was not different.

Delayed Clearance of apoE-deficient β-VLDL in 3/3 Mice—The marked increase of cholesterol-rich remnant particles seen in the 3/3 animals in response to an atherogenic diet suggests that human apoE3 is not as effective as its murine homologue in the clearance of these particles in mice. To test this possibility, we injected ^{14}C-radiolabeled remnant particles (>72% cholesterol ester) in the β-VLDL flotation range (prepared from apoE-deficient mice) into mice fed normal chow and measured the decay of label over a 4-h period. The decay of [^{14}C]cholesterol was rapid in the +/+ mice and virtually complete in 15 min (Fig. 8). The fractional catabolic rate in +/+ mice based on a single compartment system was 0.12 ± 0.002/min. Clearance of the same lipoproteins in apoE (−/−) mice was considerably slower, with a fractional catabolic rate of 0.005 ± 0.0003/min. The 3/3 mice had a rate (0.02 ± 0.0003/min) 6-fold slower than +/+ mice but more rapid than the apoE (−/−) mice. Note, however, that within 2 h the amount of label remaining in the 3/3 mice had decreased to the same levels seen in the +/+ mice.

Morphometric Evaluations of Aortic Lesions—After 3 months on an atherogenic diet, 3/3 and +/+ animals (all females) were evaluated for atherosclerotic lesions. All measurements were made from sections in the proximal aorta near the aortic valve attachment sites. All six 3/3 animals developed substantial atherosclerotic lesions with a logarithmic mean area of 6.4×10^4 μm^2 (ranging from 2.4×10^4 to 16.8×10^4). In contrast four out of five +/+ animals developed fatty streak lesions that were small, with a logarithmic mean area of 5.1×10^3 μm^2 (ranging from 2.9×10^3 to 9.2×10^3) (Fig. 9). One +/+ animal had no lesions. These observations clearly demonstrate that the 3/3 mice are much more susceptible to diet-induced atherosclerosis than +/+ mice.

DISCUSSION

We have successfully replaced the coding sequence of the mouse *apoE* gene with the equivalent human *APOE3* coding region without altering any known endogenous regulatory sequences. Expression of the human apoE mRNA in the liver, brain, and other tissues parallels that found normally in wild type mice. Thus, the human APOE3 protein is functional and is expressed at physiological levels in these modified mice, thereby providing a model for studying the function of human APOE3 *in vivo*.

To date, pronuclear injection of DNA has been used to generate transgenic animals expressing various forms of human APOE to study its role in lipid metabolism (19–24, 47). There

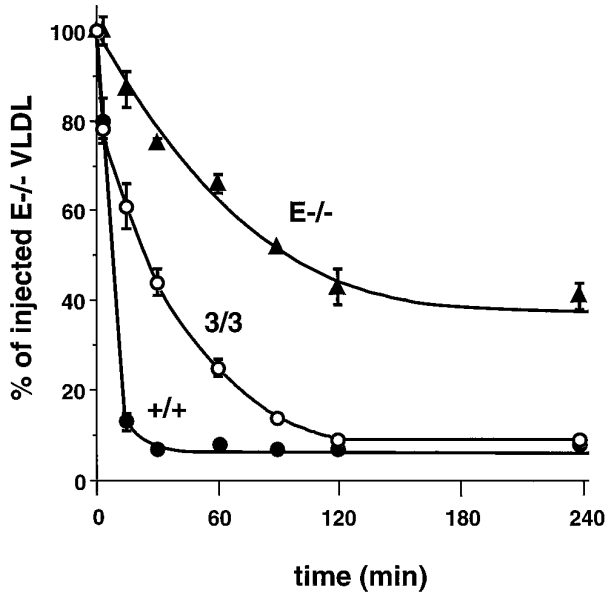

FIG. 8. **The plasma clearance of ApoE(−/−) remnant particles in controls and 3/3 mice.** Three mice of each group (▲, ApoE-deficient mice (E−/−); ●, 3/3; and ●, +/+) were injected with radiolabeled apoE(−/−) remnant particles, and its clearance was measured for 4 h. Each data point shows the mean ± S.D. Abbreviations are: *3/3*, homozygous human apoE3 mice; +/+, wild type mice; *E−/−*, apoE-deficient mice.

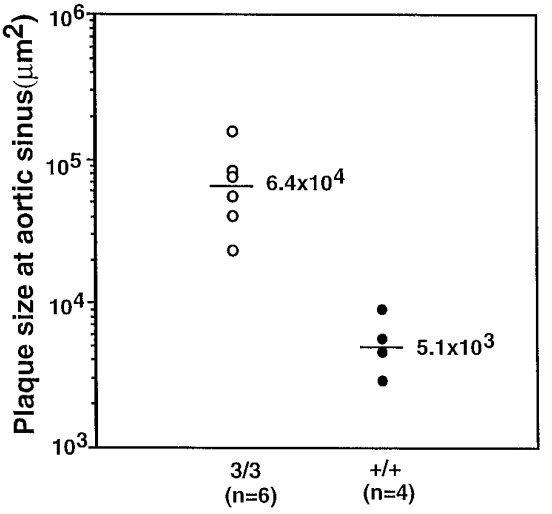

FIG. 9. **Morphometric evaluation of atherosclerotic lesions in mice fed an atherogenic diet.** All mice were F2 females kept on an atherogenic diet for 12 weeks before sacrifice. Measurements for each animal were made from a single section in the proximal aorta near the aortic valve attachment site. The logarithmic means of the lesion areas from all six 3/3 mice and four of five +/+ mice are indicated ($p = 0.006$). One +/+ mouse had no lesions.

are three severe limitations to this approach as follows: the number of copies of the transgene can vary over wide ranges; there are marked and uncontrolled differences in the expression of transgenes at different chromosomal locations; and the presence of the endogenous mouse protein complicates the interpretation of the results. Most importantly, rigorous comparisons between different isoforms are not possible because of the variable expression inherent in conventional transgenic animals.

Mice made by replacement of the endogenous mouse coding region with the equivalent region of the human gene retain the natural chromosomal context at the apoE locus. Thus, locus-specific sequences and enhancers are not altered except for any possible intragenic control sequences that differ between mice and humans. Therefore, it was expected that tissue-specific expression of the human replacement *APOE3* gene would closely parallel that of the endogenous mouse apoE gene. Our mRNA studies show that this expectation was indeed fulfilled, with the exception of intestinal apoE mRNA which was slightly reduced in the 3/3 mice compared with the +/+ mice. The significance of this reduction in intestinal expression is not clear, considering that intestinal apoE expression is very low compared with other tissues and that chylomicrons originating from the small intestine are known to contain very little apoE (34, 35). Differences between the 3/3 and +/+ mice consequently are highly informative as far as function of the apolipoprotein itself are concerned. Thus, gene replacement demonstrates the advantages over pronuclear injection in generating transgenic animals.

The lipid profiles of the 3/3 and +/+ mice are very similar when the mice are maintained on a chow (low fat) diet, and the fasting levels of total cholesterol, triglyceride, and HDL cholesterol are essentially identical in the two animals. However, when the same mice were fed a high fat diet, the 3/3 animals responded with a 5-fold increase in total cholesterol compared with a 1.5-fold increase in the +/+ animals. Second, after 3 months on a high fat diet, the atherosclerotic plaques seen in all the 3/3 animals were 13-fold larger than those observed in the wild type controls. Third, there was a 6-fold slower clearance rate of remnant lipoprotein particles in the 3/3 animals. The accumulation of cholesterol and the delayed clearance of remnant particles observed in the 3/3 animals are likely causes of the increased susceptibility to lesion development.

The dramatic delay in clearance of remnant particles in the 3/3 mice was unexpected since previous studies using transgenic mice expressing human APOE have revealed normal or enhanced clearance kinetics (22, 36). One possible explanation for the observed delay in clearance is that the human APOE3 protein has a lower affinity to mouse LDLR and/or other receptors than mouse ApoE because of species differences in their structures. Mouse and human apoE differ in 30% of their amino acid sequences with most of the differences being at the amino and carboxyl termini (1). The receptor binding domain (residues 136–160) is highly conserved between mouse and human apoE since 21 of 25 residues are identical in this region including seven residues designated as critical for receptor binding (37, 38). The residues that differ have conservative substitutions (*e.g.* methionine for leucine) that do not affect the net charge or hydrophobicity of the protein and would not be predicted to have any substantial effects on the protein conformation (39). Thus, it must be ascribed to differences outside the receptor binding domain if the affinity for the receptor differs between the mouse and human apoE proteins. Species differences in the receptors that interact with apoE, such as the LDLR, and low density lipoprotein receptor-related protein, could also contribute to a lower affinity.

A dysfunctional interaction between human APOE3 and mouse heparan sulfate proteoglycans (HSPG) may also contribute to the delay in clearance. It has been postulated that HSPG's are involved in the initial sequestration process that enhances the uptake of apoE containing lipoproteins (40, 41). The interaction of apoE with HSPG's is thought to occur mainly via electrostatic attraction (42). Human APOE3 has a cysteine at position 112 where the mouse protein has an arginine at the equivalent position (mouse apoE residue 104). This charge difference could be significant, even though residue 112 is outside the known heparin-binding domain.

The delayed clearance could also be due to protein-protein interactions not involving receptors. Several proteins are

known to interact with apoE and play a role in lipid metabolism. For example, the interaction of apoE with hepatic and lipoprotein lipases mediates/or enhances the catabolism of lipoproteins (41). Lipoprotein particles containing human APOE3 may be less efficient in this type of interaction than mouse ApoE. This would have important consequences in the remodeling and processing phase of lipoprotein catabolism.

Another consideration in the clearance experiment is that the exogenously introduced remnant particles have to acquire apoE prior to their removal by receptors. In +/+ mice most of the plasma apoE is associated with HDL particles that are presumably the source of apoE used to clear the exogenously added remnants. In the 3/3 animals, however, the majority of plasma apoE3 is associated with large lipoproteins and may not transfer as easily to exogenously added particles. In support of this, we and others (27) have noted that the distributions of apoE among mouse plasma lipoproteins analyzed by FPLC and by ultracentrifugation do not always agree and that apoE associated with HDL are more readily lost by ultracentrifugation. Although the capacity for apoE3 to exchange between different classes of lipoproteins has not been documented, the decreased ability of apoE3 to transfer from large lipoproteins may have important implications.

The association of apoE3 with larger lipoproteins in mice (Fig. 5, *A* and *C*) is different from observations made in humans that demonstrate a preference of apoE3 for HDL (1, 43). It is very unlikely that this difference is the result of a mutation unexpectedly introduced into the *APOE3* gene during its manipulation because in our work[2] we observed that transgenic apoE3 mice, in an endogenous apoE (−/−) background, had a virtually identical apoE3 distribution pattern as seen in the 3/3 replacement mice. These mice were made by pronuclear injection of a human cosmid clone isolated from a different individual from the one we used to make our mice (24). Similar findings were also reported by Taylor *et al.* (44) in transgenic apoE3 mice (that also express mouse apoE) which showed that the majority of human APOE3 resided in larger lipoprotein particles using SDS-PAGE immunoblot analysis of fractions separated by sequential density ultracentrifugation. In this work the authors also found that mouse ApoE and human APOE co-distributed among lipoproteins. This is different from the results of our FPLC analysis of 3/+ heterozygote plasma which shows that approximately half of the mouse ApoE and only a minor fraction of human APOE3 was associated with HDL (data not shown). It is not known whether the observed differences between our work and Taylor *et al.* are the result of different techniques used to fractionate the plasma lipoproteins or the result of different levels of human APOE and mouse ApoE expression in the two types of mice. Further characterization of these large apoE3-rich lipoprotein particles is required to understand the observed delay in clearance in the 3/3 animals.

The reduced clearance rate of remnant particles in the 3/3 mice, whatever its cause eventually proves to be, is not sufficient to cause any alteration in fasted plasma cholesterol levels in these animals relative to their +/+ littermates when the animals are on a normal chow diet. The 3/3 mice are, however, much more susceptible to diet-induced hyperlipidemia and atherosclerosis than their +/+ littermates. Possibly, on the high fat diet a postprandial accumulation of β-VLDL's occurs that leads to the development of atherosclerosis, as suggested by Zilversmit (45). In human *APOE2* homozygous individuals with type III hyperlipoproteinemia, there is an abnormal accumulation of remnant particles that has been suggested to cause accelerated coronary and peripheral vascular disease (46). Even small changes in lipid metabolism that decrease the clearance efficiency of lipoproteins are likely to have dramatic effects on the development of atherosclerosis, and thus the 3/3 animals give us an opportunity to investigate what changes are important.

In conclusion, we have demonstrated the use of targeted gene replacement to generate mice expressing the most common human isoform, APOE3, at physiological levels. These mice allow us to document the behavior of the human APOE3 isoform *in vivo* in mice without any co-expression of mouse apoE. Future experiments comparing these mice with mice expressing the human apoE2 and E4 isoforms created in an identical manner should prove invaluable for studying diseases related to the different human apoE isoforms.

Acknowledgments—We thank Dr. Masahiko Watanabe for his help in building the targeting construct and Daniel Throckmorton, Brian Oswald, Denise Lee, and Kim Kluckman for their technical help. We also thank Dr. J. Taylor for the apoE3 plasmid, Dr. J. C. Fruchart for the E01 antibody, Dr. S. Young for the anti-mouse ApoB sera, Dr. N. Rifai for validation of our human apoE standard, and Dr. O. Smithies, Dr. H. deSilva, and Dr. S. Kirby for reviewing the manuscript.

[2] P. M. Sullivan and N. Maeda, unpublished observations.

REFERENCES

1. Weisgraber, K. H. (1994) *Adv. Protein Chem.* **45,** 249–302
2. Herz, J., Hamann, U., Rogne, S., Myklebost, O., Gausepohl, H., and Stanley, K. K. (1988) *EMBO J.* **7,** 4119–4127
3. Mahley, R. W., and Innerarity, T. L. (1977) *J. Biol. Chem.* **252,** 3980–3986
4. Mahley, R. W. (1978) in *Disturbances in Lipid and Lipoprotein Metabolism* (Dietschy, J. M., Gotto, A. M., Jr., and Ontko, J. A., eds) pp. 181–197, American Physiological Society, Bethesda
5. Olaisen, B., Teisberg, P., and Gedde-Dahl, T., Jr. (1982) *Hum. Genet.* **62,** 233
6. Kardassis, D., Laccotripe, M., Talianidis, I., and Zannis, V. (1996) *Hypertension* **27,** 980–1008
7. Paik, Y.-K., Chang, D. J., Reardon, C. A., Walker, M. D., Taxman, E., and Taylor, J. M. (1988) *J. Biol. Chem.* **263,** 13340–13349
8. Smith, J. D., Melian, A., Leff, T., and Breslow, J. L. (1988) *J. Biol. Chem.* **263,** 8300–8308
9. Simonet, W. S., Bucay, N., Lauer, S. J., and Taylor, J. M. (1993) *J. Biol. Chem.* **268,** 8221–8229
10. Blue, M. L., Williams, D. L., Zucker, S., Khan, S. A., and Blum, C. B. (1983) *Proc. Natl. Acad. Sci. U. S. A.* **80,** 283–287
11. Basu, S. K., Ho, Y. K., Brown, M. S., Bilheimer, D. W., Anderson, R. G. W., and Goldstein, J. L. (1982) *J. Biol. Chem.* **257,** 9788–9795
12. Hallman, D. M., Boerwinkle, E., Saha, N., Sandholzer, C., Menzel, H. J., Császár, A., and Utermann, G. (1991) *Am. J. Hum. Genet.* **49,** 338–349
13. Rall, S. C., Jr., Weisgraber, K. H., and Mahley, R. W. (1982) *J. Biol. Chem.* **257,** 4171–4178
14. Weisgraber, K. H., Innerarity, T. L., and Mahley, R. W. (1982) *J. Biol. Chem.* **257,** 2518–2521
15. Utermann, G. (1982) *La Ricerca Clin. Lab.* **12,** 23–33
16. Boerwinkle, E., Visvikis, S., Welsh, D., Steinmetz, J., Hanash, S. M., and Sing, C. F. (1987) *Am. J. Hum. Genet.* **27,** 567–582
17. Schmechel, D. E., Saunders, A. M., Strittmatter, W. J., Crain, B. J., Hulette, C. M., Joo, S. H., Pericak-Vance, M. A., Goldgaber, D., and Roses, A. D. (1993) *Proc. Natl. Acad. Sci. U. S. A.* **90,** 9649–9653
18. Saunders, A. M., Strittmatter, W. J., Schmechel, D., George-Hyslop, S. T., Pericak-Vance, M. A., Joo, S. H., Rosi, B. L., Gusella, J. F., Crapper-MacLachlan, D. R., Albert, M. J., Hulette, C., Crain, B., Goldgaber, D., and Roses, A. D. (1993) *Neurology* **43,** 1467–1472
19. Smith, J. D., Plump, A. S., Hayek, T., Walsh, A., and Breslow, J. L. (1990) *J. Biol. Chem.* **265,** 14709–14712
20. Simonet, W. S., Bucay, N., Lauer, S. J., Wirak, D. O., Stevens, M. E., Weisgraber, K. H., Pitas, R. E., and Taylor, J. M. (1990) *J. Biol. Chem.* **265,** 10809–10812
21. Fazio, S., Horie, Y., Simonet, W. S., Weisgraber, K. H., Taylor, J. M., and Rall, S. C., Jr. (1994) *J. Lipid Res.* **35,** 408–416
22. Mortimer, B.-C., Redgrave, T. G., Spangler, E. A., Verstuyft, J. G., and Rubin, E. M. (1994) *Arterioscler. Thromb.* **14,** 1542–1552
23. van den Maagdenberg, A. M. J. M., Hofker, M. H., Krimpenfort, P. J. A., de Bruijn, I., van Vlijmen, B., van der Boom, H., Havekes, L. M., and Frants, R. R. (1993) *J. Biol. Chem.* **268,** 10540–10545
24. Xu, P.-T., Schmechel, D., Rothrock-Christian, T., Burkhart, D. S., Qiu, H-L., Popko, B., Sullivan, P. M., Maeda, N., Saunders, A. M., Roses, A. D., and Gilbert, J. R. (1996) *Neurobiol. Dis.* **3,** 229–245
25. Tybulewicz, V. L. J., Crawford, C. E., Jackson, P. K., Bronson, R. T., and Mulligan, R. C. (1991) *Cell* **65,** 1153–1163
26. Koller, B. H., Kim, H.-S., Latour, A. M., Brigman, K., Boucher, R. C., Jr., Scrambler, P., Wainwright, B., and Smithies, O. (1991) *Proc. Natl. Acad. Sci. U. S. A.* **88,** 10730–10734
27. de Silva, H. V., Más-Oliva, J., Taylor, J. M., and Mahley, R. W. (1994) *J. Lipid Res.* **35,** 1297–1310
28. Chomczynski, P., and Sacchi, N. (1987) *Anal. Biochem.* **162,** 156–159
29. Thomas, P. S. (1980) *Proc. Natl. Acad. Sci. U. S. A.* **77,** 5201–5205
30. Leroy, A., Vu-dac, N., Koffigan, M., Clavey, V., and Fruchart, J. C. (1988)

J. Immunoassay **9,** 309–334
31. Quarfordt, S. H., Oswald, B., Xu, H. S., Zhang, S., and Maeda, N. (1995) *J. Lipid Res.* **36,** 1227–1235
32. Zhang, S. H., Reddick, R. L., Burkey, B., and Maeda, N. (1994) *J. Clin. Invest.* **94,** 937–945
33. Green, E. K., Bain, S. C., Day, P. J. R., Barnett, A. H., Charelson, F., Jones, A. F., and Walker, M. R. (1991) *Clin. Chem.* **37,** 1263–1268
34. Robinson, S. F., and Quarfordt, S. H. (1978) *Biochim. Biophys. Acta* **541,** 492–503
35. Imaizumi, K., Fainaru, M., and Havel, R. J. (1978) *J. Lipid Res.* **19,** 712–722
36. de Silva, H. V., Lauer, S. J., Wang, J., Simonet, W. S., Weisgraber, K. H., Mahley, R. W., and Taylor, J. M. (1994) *J. Biol. Chem.* **269,** 2324–2335
37. Yang, Y.-W., Chan, L., and Li, W.-H. (1991) *J. Mol. Evol.* **32,** 469–475
38. Wardell, M. R., Brennan, S. O., James, E. D., Fraser, R., and Carrell, R. W. (1987) *J. Clin. Invest.* **80,** 483–490
39. Lalazar, A., Weisgraber, K. H., Rall, S. C., Jr., Giladi, H., Innerarity, T. L., Levanon, A. Z., Boyles, J. K., Amit, B., Gorecki, M., Mahley, R. W., and Vogel, T. (1988) *J. Biol. Chem.* **263,** 3542–3545
40. Landis, B. A., Rotolo, F. S., Meyers, W. C., Clark, A. B., and Quarfordt, S. H. (1987) *Am. J. Physiol.* **252,** C805–C810
41. Mahley, R. W., and Hussain, M. M. (1991) *Curr. Opin. Lipidol.* **2,** 170–176
42. Mahley, R. W., Weisgraber, K. H., and Innerarity, T. L. (1979) *Biochim. Biophys. Acta* **575,** 81–91
43. Weisgraber, K. H. (1990) *J. Lipid Res.* **31,** 1503–1511
44. Taylor, J. M., Simonet, W. S., Bucay, N., Lauer, S. J., and de Silva, H. V. (1991) *Curr. Opin. Lipidol.* **2,** 73–80
45. Zilversmit, D. B. (1979) *Circulation* **60,** 473–485
46. Slyper, A. H. (1992) *Lancet* **340,** 289–291
47. van Vlijmen, B. J. M., van Dijk, K. W., van't Hof, H. B., van Gorp, P. J. J., van der Zee, A., van der Boom, H., Breuer, M. L., Hofker, M. H., and Havekes, L. M. (1996) *J. Biol. Chem.* **271,** 30595–30602